Mechanical properties up to 1900 K of $Al_2O_3/Er_3Al_5O_{12}/ZrO_2$ eutectic ceramics grown by the laser floating zone method

M.C. Mesa , P.B. Oliete , J.Y. Pastor , A. Martín , J. LLorca

Abstract

Directionally solidified Al_2O_3–$Er_3Al_5O_{12}$–ZrO_2 eutectic rods were processed using the laser floating zone method at growth rates of 25, 350 and 750 mm/h to obtain microstructures with different domain size. The mechanical properties were investigated as a function of the processing rate. The hardness, ~15.6 GPa, and the fracture toughness, ~4 MPa $m^{1/2}$, obtained from Vickers indentation at room temperature were practically independent of the size of the eutectic phases. However, the flexural strength increased as the domain size decreased, reaching outstanding strength values close to 3 GPa in the samples grown at 750 mm/h. A high retention of the flexural strength was observed up to 1500 K in the materials processed at 25 and 350 mm/h, while superplastic behaviour was observed at 1700 K in the eutectic rods solidified at the highest rate of 750 mm/h.

Keywords: $Al_2O_3/Er_3Al_5O_{12}/ZrO_2$; Directionally solidified eutectic ceramics; Mechanical properties; High temperature

1. Introduction

Tailoring the microstructure of ceramic composites is an interesting route to extend their potential applications. Full-dense ceramic composites can be obtained by directional solidification of ceramic oxide eutectics from the melt. Eutectic growth allows a homogeneous mixing of the phases and the phase size can be controlled with the solidification rate, following the Hunt-Jackson law: $\lambda \propto v^{-1/2}$, with λ the interphase spacing and v the growth rate.[1] Reduction of the microstructure characteristic size into the nm range can lead to unusual structural and functional properties.[2]

In the field of structural materials, directionally solidified eutectics (DSE) based in Al_2O_3 are candidates for thermomechanical applications at high temperature due to their good creep resistance and microstructural stability.[2,3] In particular, binary and ternary eutectics from the Al_2O_3–ZrO_2–Y_2O_3 system have been investigated because of their excellent mechanical properties.[4–7] Recently, a strong dependence of the flexural strength of Al_2O_3–$Y_3Al_5O_{12}$ eutectic rods with the phase size was reported,[8] and outstanding mechanical properties were attained in nanostructured Al_2O_3–$Y_3Al_5O_{12}$–ZrO_2 eutectics with fibrillar microstructure.[9]

The application field of these materials can be extended with the addition to the eutectic composition of rare earth oxides as Er_2O_3. Rare earth ions in crystals emit radiation in narrow bands, allowing their use as selective emitters even at high temperature. In the case of Er^{3+} ion, Al_2O_3–$Er_3Al_5O_{12}$ eutectic becomes a selective emitter very suitable for thermophotovoltaic systems as a result of the spectral matching of its emission band with the sensitive region of the GaSb photoconverter.[10]

Both structural and functional properties make of these materials an interesting subject of investigation and recent studies have been carried out in DSE of the system Al_2O_3–Er_2O_3.[11–16] Optimization of the mechanical properties of these eutectics can be achieved with finer microstructures due to the strong dependence of the mechanical properties of the directionally solidified Al_2O_3-based eutectics with the size of the microstructure. Increasing the number of components to the melt and high growth rates can result in a large reduction in the size of the eutectic domains.[9]

In this work, the ternary system Al_2O_3–ZrO_2–Er_2O_3 was studied. Directionally solidified ternary eutectic rods were processed using the laser heated floating zone (LFZ) method.

This processing technique achieves very large thermal gradients at the liquid/solid interface and therefore, high growth rates can be used. The hardness, fracture toughness and flexural strength, of these eutectics were investigated as a function of the growth rate together with the evolution of the flexural strength with temperature up to 1900 K.

2. Experimental details

Eutectic rods of Al_2O_3–$Er_3Al_5O_{12}$–ZrO_2 were fabricated by the LFZ technique. Ceramics were prepared with a mixture of commercial powders of Er_2O_3 (Aldrich, 99.99%), Al_2O_3 (Sigma–Aldrich, 99.99%) and ZrO_2 (Aldrich 99%) in the eutectic composition: 65.9 mol% Al_2O_3, 15.5 mol% Er_2O_3, 18.6 mol% ZrO_2.[17] Precursor rods were prepared by isostatically pressing the powder for 3 min at 200 MPa. They were sintered in a furnace at 1500 °C during 12 h.

Directional solidification of the rods was carried out with the LFZ method using a CO_2 laser and growth rates of 25, 350 and 750 mm/h. Different densification stages were applied at low growth rate (100–250 mm/h) to eliminate the precursor porosity. The last stage was always performed with the grown crystal travelling downwards and without rotation of the crystal or precursor. Experiments were performed in nitrogen atmosphere with a slight overpressure of 0.1–0.25 bar with respect to ambient pressure to reduce the porosity in the solidified rod.[18] Typical diameters of the processed rods were in the range 0.8–1.5 mm. The different materials will be referred to using the acronym AEZ*x*, where *x* is the growth rate.

The microstructure was studied from back-scattered electron images obtained in a Merlin Field Emission Scanning Electron Microscopy (FESEM) from Carl Zeiss (Germany) on cut and polished transverse and longitudinal cross-sections of the grown rods.

The Vickers hardness was measured following the ASTM C1327-99 Standard using a microhardness tester Matsuzawa, MXT 70, with an indentation load of 4.9 N and a holding time of 15 s. At least 10 valid indentations were made on polished transverse and longitudinal cross sections of each sample. The fracture toughness was determined by the indentation technique. The crack lengths were measured using an optical microscope.

The bending strength of the rods at room temperature was determined from three-point flexural tests performed in air in a servomechanical testing machine (model 4505 Instron Ltd., UK) with a loading span of 8.5 mm length. The tests were performed on the as-grown rods of ~1 mm in diameter and using a crosshead speed of 100 μm/min. The specimen and the loading fixture were placed in a furnace and loaded through two alumina rods connected to the actuator and load cell, respectively, for the high temperature tests. The heating rate was 10 K/min up to 1300 K, 5 K/min up to 1500 K, 3 K/min up to 1750 K, and 1 K/min above this point. The specimen was held at the test temperature for 30 min before testing.

3. Results and discussion

3.1. Microstructure

Eutectic AEZ rods were obtained by directional solidification using the LFZ technique at different growth rates. All the samples presented a homogeneous and pore-free microstructure throughout the entire cross section with the exception of several colonies which were observed in the centre of the rods processed at 350 and 750 mm/h. Fig. 1(a)–(f) depicts backscattered SEM micrographs of the transverse and longitudinal cross sections from the samples grown at 25 mm/h, 350 mm/h and 750 mm/h. The three phases present in the eutectic were Al_2O_3 (dark contrast), $Er_3Al_5O_{12}$ (Erbia aluminum garnet, EAG, grey contrast)

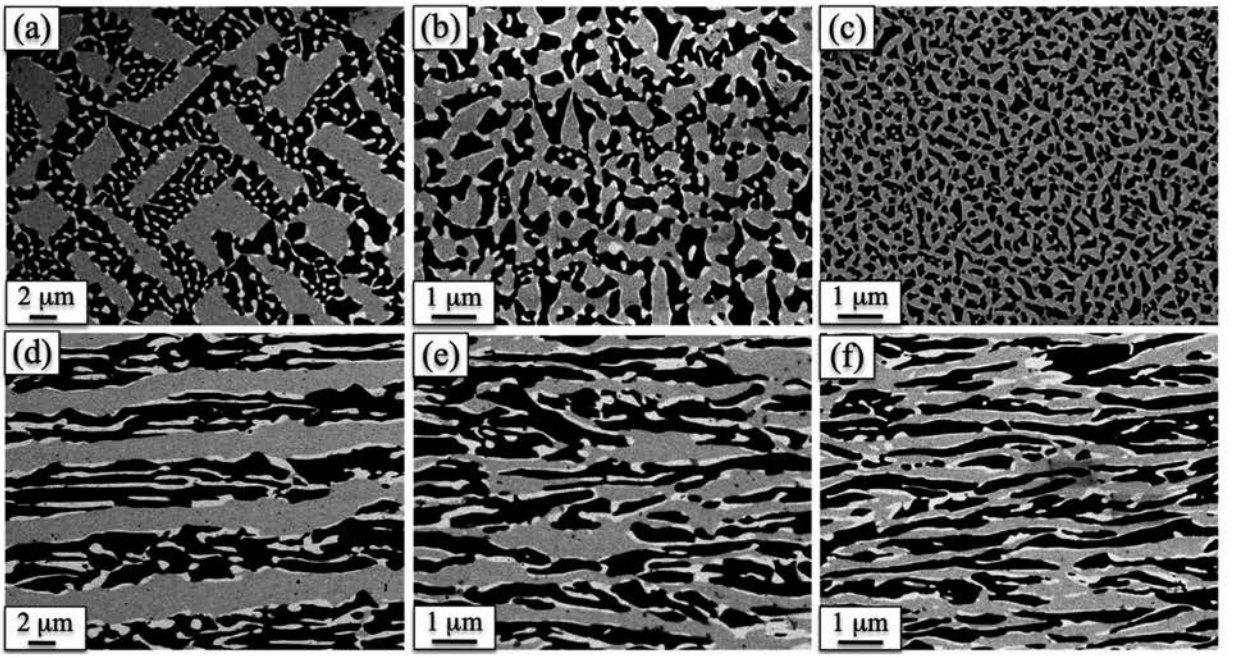

Fig. 1. SEM micrographs of the transverse and longitudinal cross-sections, respectively, of AEZ25 (a)–(d), AEZ350 (b)–(e) and AEZ750 (c)–(f).

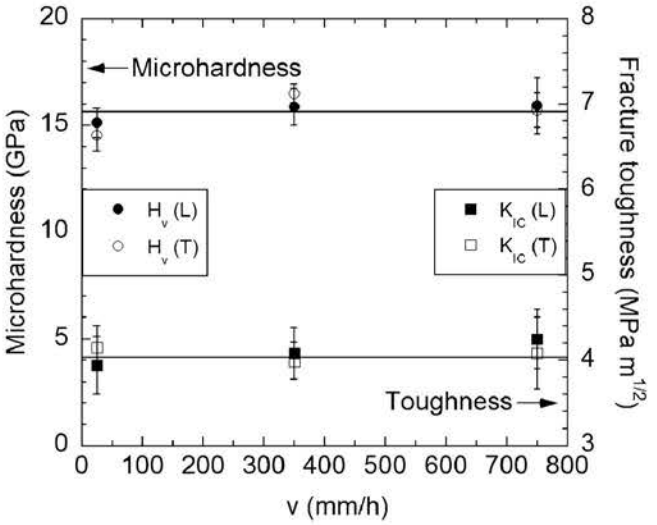

Fig. 2. Microhardness (O) and fracture toughness (□) of Al_2O_3–$Er_3Al_5O_{12}$–ZrO_2 eutectic rods as a function of the growth rate. Open symbols correspond to measures on a transverse cross section (*T*) and solid symbols on a longitudinal cross section (*L*).

and fully-stabilized cubic Er_2O_3-doped ZrO_2 (white contrast). The volume fraction of the phases obtained using area analysis of SEM images were $39 \pm 1\%$, $40 \pm 1\%$ and $21 \pm 1\%$, for Al_2O_3, $Er_3Al_5O_{12}$ and ZrO_2, respectively. These values are close to the volume fractions calculated using the eutectic composition.[19]

The size of the phases and the morphology of the microstructure were highly dependent of the solidification rate. For rods grown at 25 mm/h, the microstructure adopted a pattern consisting of a geometrical network of the two major eutectic phases, Al_2O_3 and $Er_3Al_5O_{12}$, with the ZrO_2 phase embedded in the Al_2O_3 and at the Al_2O_3–EAG interfaces (Fig. 1(a)). This geometrical pattern changed at 350 and 750 mm/h to an irregular interpenetrated microstructure of the three phases (Fig. 1(b) and (c)). In all samples, the phases were elongated along the growth direction (Fig. 1(d)–(f)) and their sizes were controlled by the solidification parameters, decreasing when the growth rate increases. The thickness of the $Er_3Al_5O_{12}$ domains was in the range 1.6–2.5 μm at 25 mm/h and decreased up to 0.15–0.22 μm at 750 mm/h. The ternary eutectic microstructure was finer that the obtained for the binary eutectic Al_2O_3–$Er_3Al_5O_{12}$[12] at the same solidification rates, as expected by the incorporation of more components to the eutectic mixture.[9]

3.2. Hardness and fracture toughness

Hardness in ternary eutectic rods was measured from microhardness Vickers tests performed in longitudinal and transverse cross sections in AEZ25, AEZ350 and AEZ750 rods at room temperature. Fig. 2 shows the average microhardness plotted as a function of the growth rate. The hardness varied between 14.5 GPa and 16.5 GPa, very close to the values obtained for the binary eutectic Al_2O_3–$Er_3Al_5O_{12}$[12,15] and other Al_2O_3-based DSE.[8,20,21]. The hardness was equivalent in the transverse and longitudinal cross sections and decreased slightly in the samples grown at the lowest solidification rate. A stronger dependence on the growth rate was reported for the ternary eutectic of the system Al_2O_3–ZrO_2–Y_2O_3.[7,22]

Fracture toughness was determined using the indentation technique on the samples prepared for Vickers hardness testing at room temperature. Although numerous test techniques are reported in the literature to measure the fracture toughness in ceramics, the indentation method presents the advantages of simplicity and economy in addition to the small size of specimen. Recently, some works have critically revised the use of this technique to determine the absolute fracture toughness.[23] However, the indentation method is suited to toughness evaluation on a comparative basis,[20,24] as in the present study, where the influence of the solidification rate or the inclusion of a component in the eutectic mixture is investigated.

Well-defined cracks emerged from the corners of the Vickers indentation in AEZ samples. In the case of transverse cross sections, the crack pattern was symmetric for all the solidification rates, in good agreement with the isotropy of the microstructure in such orientation (Fig. 3(a)). However, the crack length parallel to the growth direction was often slightly longer in the longitudinal cross section, pointing to the interaction of the crack with the anisotropic microstructure (Fig. 1(d)–(f)). Crack propagation was preferentially transgranular, as a consequence of the strong bonding between phases, although some intergranular fracture was also observed. Crack arrest, followed by the development of another parallel crack, was occasionally observed throughout the crack path (Fig. 3(b)).

The fracture toughness was calculated from the crack length. Different equations are reported in the literature for evaluating material toughness from the indentation method depending of the type of cracks developed. Two major types of cracks are formed: median-radial cracks, which completely surround the indentation, and Palmqvist cracks, which form laterally on planes closely parallel to the surface. It has been proposed that Palmqvist cracks develop at lower values of the ratio of crack-to-indent size than the median-radial cracks.[25] For the AEZ rods, the Niihara condition for the Palmqvist cracks $0 \leq l/a \leq 2.5$ was fulfilled, with l, the crack length measured from the corner of the indentation and a, half the indentation diagonal. Therefore, the calculation of the fracture toughness was carried out using the equation proposed by Niihara et al.:[25]

$$K_{IC} = 0.035\left(\frac{H}{E}\right)^{-2/5}\left(\frac{l}{a}\right)^{-1/2} Ha^{1/2}\phi^{-3/5} \quad (1)$$

where E is the Young modulus of the material, H is the Vickers hardness, and $\phi \cong 3$ a constrain factor. The Young modulus for the ternary eutectic was taken 315 GPa, as calculated from the rule of mixtures parallel to the growth direction.

Fig. 2 shows the average value of the fracture toughness in AEZ rods determined using Eq. (1) in both longitudinal and transverse cross sections as a function of the solidification rate. The fracture toughness was found to be independent of the growth rate in both orientations. The K_{IC} perpendicular to the growth direction (4.1 MPa m$^{1/2}$) was slightly higher than the one parallel to the growth axis (3.8 MPa m$^{1/2}$), in agreement with the interaction of the crack path with the anisotropic

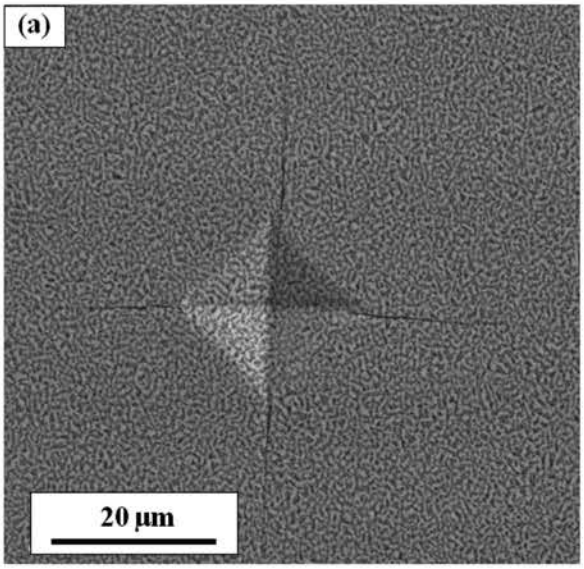

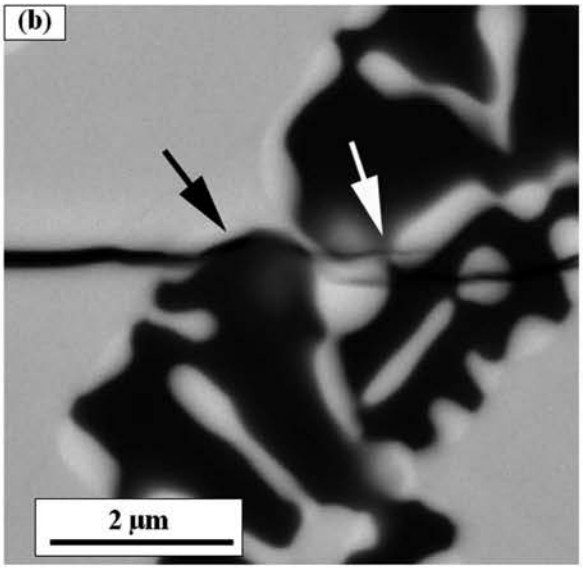

Fig. 3. (a) Cracking pattern in a transverse cross section of AEZ350 under an indentation loading of 4.9 N. (b) Crack propagation in a transverse cross section of AEZ25 where crack arrest and intergranular fracture are marked with arrows.

microstructure. The results here reported can be compared with those obtained with the same technique in the binary DSE Al_2O_3–YAG[8] and Al_2O_3–EAG,[12] which present a fracture toughness of $\sim 2\,MPa\,m^{1/2}$. Therefore, the presence of the Er_2O_3-doped ZrO_2 improved the fracture toughness by a factor 2 with respect to the binary system. The toughening effect of the zirconia has been previously reported in several ternary systems.[7,13]. The higher crack propagation resistance in ternary systems with respect to the binary systems can be tentatively attributed to the residual stresses developed upon solidification in the eutectic.[26] The thermoelastic residual stresses generated at room temperature in the ternary eutectic are higher than those in the binary system, due to the large difference in the thermal expansion between the ZrO_2 and Al_2O_3 which can lead to a stronger interaction with the interphases and give rise to crack deflection[27] and crack arrest.

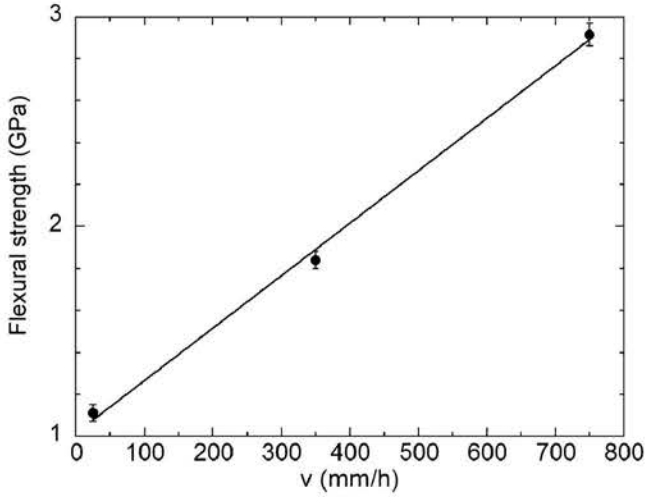

Fig. 4. Flexural strength at room temperature of AEZ eutectic rods as a function of the solidification rate.

3.3. Flexural strength

The flexural strength of the AEZ25, AEZ350 and AEZ750 rods was measured from 300 K to 1900 K. At room temperature all the samples showed linear load–displacement behaviour and brittle fracture. The strength was calculated from the maximum load in the test using the standard beam theory.

Fig. 4 shows the average flexural strength plotted as a function of the growth rate at room temperature. Contrary to hardness and fracture toughness, the flexural strength increased with the growth rate from 1.1 GPa for rods grown at 25 mm/h up to 2.9 GPa for those processed at 750 mm/h. This latter value stands as one of the highest reported in the literature for Al_2O_3-based DSE eutectics. The influence of the growth rate on the flexural strength has been previously found in other directionally solidified Al_2O_3-based eutectic such as Al_2O_3–$Y_3Al_5O_{12}$[8] and Al_2O_3–Er_2O_3.[12] The strengthening effect of the growth rate can be explained in microstructure terms, due to the strong dependence of the phase size with this processing parameter.[1] The strength of these brittle materials is controlled by the critical defect size and the resistance to crack propagation through the relation $\sigma_f \propto K_{IC}/\sqrt{a_c}$,[8] with σ_f, the flexural strength, K_{IC} the fracture toughness and a_c, the critical defect size. As discussed above, the fracture toughness in these eutectics is practically independent on the processing rate. Therefore, the magnitude limiting the strength will be the critical defect size which is largely dependent on the microstructure, in particular on the domain size.[8] Thus, the finer microstructure of the eutectic solidified at 750 mm/h gives rise to the rod with smallest flaws and, consequently, with the highest flexural strength. It should be noted that these ternary eutectics show higher strength than the corresponding Al_2O_3–$Er_3Al_5O_{12}$ binary eutectic processed at the same growth rates.[12] The advantage of the ternary system is that the addition of ZrO_2 to the eutectic mixture produces a refinement of the microstructure and thus a reduction in the flaw size.

In order to study the retention of the strength with the temperature, bending tests were performed at 1300 K, 1500 K,

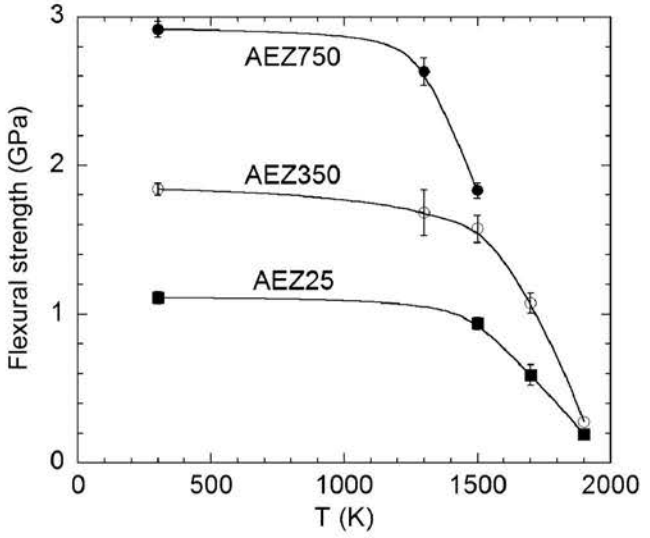

Fig. 5. Flexural strength of AEZ25 (■), AEZ350 (O) and AEZ750 (●) as a function of the temperature.

1700 K and 1900 K. Fig. 5 shows the average flexural strength plotted as a function of the temperature for all the solidification rates. The load–displacement curve was linear until failure in the samples grown at 25 and 350 mm/h and no evidence of macroscopic plastic deformation was observed even at the highest temperature. For both solidification rates, the strength retention was very good up to 1500 K, and decreased rapidly above this temperature up to one half the room temperature flexural strength at 1700 K. A similar strength drop at temperatures above 1500 K has been recently observed in directionally solidified Al_2O_3–$Y_3Al_5O_{12}$–ZrO_2 eutectics.[7,27] On the contrary, a high strength retention[8,11] was reported at temperatures of 1900 K and 2073 K in the binary Al_2O_3–$Y_3Al_5O_{12}$ and Al_2O_3–$Er_3Al_5O_{12}$ eutectics, respectively, that is, at temperatures close to its melting point. In the binary case, the three-dimensional interpenetrated network of Al_2O_3 and $Y_3Al_5O_{12}$ or $Er_3Al_5O_{12}$ phases and the high resistance to creep of the garnet limited the plastic deformation of the alumina at high temperatures.[5,14] It should be noted that the ternary eutectics grown by Bridgman at low solidification rates showed larger strength retentions with the temperature[6,17] than the rods studied here.

Several mechanisms could be the responsible for the reduction of the flexural strength with temperature in AEZ25 and AEZ350. Firstly, the release of the thermal residual stresses at high temperature could reduce the fracture toughness of the material. These thermoelastic stresses, as discussed above, are greater in the ternary than in the binary system due to the large ZrO_2 thermal expansion. Pastor et al.[28] measured the fracture toughness in Al_2O_3–$Y_3Al_5O_{12}$ and Al_2O_3–$Y_3Al_5O_{12}$–ZrO_2 DSE as a function of the temperature and a significant reduction was reported for the ternary eutectic at 1500 K, whereas no decrease was measured in the binary counterpart. Therefore, the strength of the ternary eutectic could be affected by the reduction in the fracture toughness as a result of the relief of the residual stresses at high temperature. Secondly, diffusion

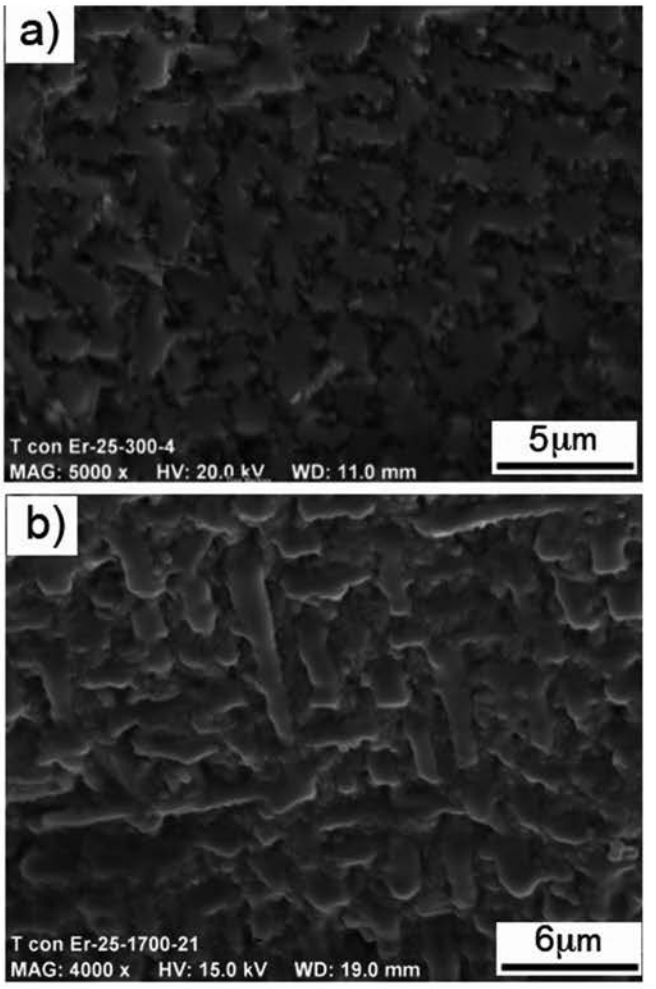

Fig. 6. Fracture surfaces of AEZ25 rods tested at (a) 300 K and (b) 1700 K.

processes, due to their smaller domain size and lower eutectic temperature, could also influence the strength of the ternary eutectic. Thirdly, the growth of the defects due to the homogeneous coarsening of the microstructure with the temperature could also play a role. This phenomenon was almost absent in the binary eutectics because of their coarser microstructure at room temperature.[11] A very small degradation of the flexural strength was observed with the temperature in the binary Al_2O_3–$Y_3Al_5O_{12}$ eutectic[8] and only in the material grown at the highest rates because of the smaller phase size that favoured the coarsening. This phenomenon was not negligible in the ternary system and led to a significant reduction in the strength. Finally, the presence of cubic ZrO_2 is another factor that can contribute to the strength degradation in the Al_2O_3–$Er_3Al_5O_{12}$–ZrO_2 eutectics as its resistance to plastic deformation is lower than that of alumina and garnet crystals. Single crystal of cubic ZrO_2 readily shows plastic deformation at temperatures above 1500 K which can decrease the strength of the rods at high temperatures.

The fracture surfaces of AEZ25 specimens tested at 300 K and 1700 K are shown in Fig. 6(a) and (b), respectively. The geometrical pattern, typical of this solidification rate (Fig. 1(a)), is clearly visible on both fracture surfaces. The fracture surfaces were flat at both temperatures, indicating that fracture was brittle,

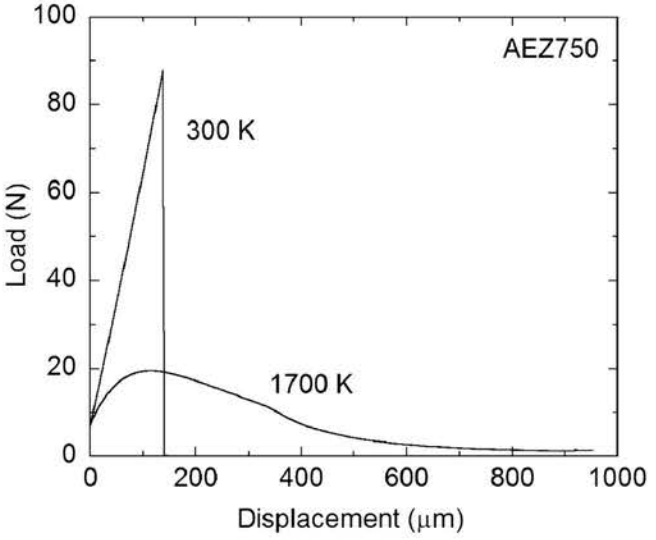

Fig. 7. Load–displacement curve obtained from flexural tests for AEZ750 at 300 K and 1700 K.

and the large EAG domains showed transgranular fracture. The main difference observed in the fracture surfaces between 300 K and 1700 K was the rounding of the eutectic domains at 1700 K, and this can be attributed to the coarsening of the microstructure at high temperature.

The flexural strength of the samples grown at 750 mm/h also showed a high retention up to 1300 K. However, the flexural behaviour at temperatures above 1500 K differs from that observed for rods grown at lower solidification rates. Instead of the abrupt strength reduction observed for AEZ25 and AEZ350, large plastic deformations were found when the rods were tested at 1700 K and above. Fig. 7 shows the load–displacement curve obtained from flexural tests at 300 K and 1700 K for the sample processed at 750 mm/h. While the typical linear elastic behaviour was obtained at room temperature, large plastic deformations were observed at 1700 K. Plastic deformation in Al_2O_3-based DSE at high temperatures has been previously reported. A ductile behaviour was observed at 1873 K in directionally solidified Al_2O_3–$GdAlO_3$ eutectic ceramics, which was attributed to dislocation motion.[29] Recently, a superplastic behaviour was found in Al_2O_3–$Y_3Al_5O_{12}$–ZrO_2 nanofibrilar eutectics. No evidence of dislocation activity was found in any of the three eutectic phases and the large plastic deformation was attributed to the mass transport by diffusion.[30] In the same way, we have attributed the plastic deformation observed in Al_2O_3–$Er_3Al_5O_{12}$–ZrO_2 eutectic rods to diffusion based-mechanisms rather than dislocation motion. We should note that dislocation activity should be higher in the ceramics processed at low growth rates, with coarser microstructure. However, no evidence of plastic deformation was observed in AEZ25 and AEZ350. The small size of the eutectic phases in AEZ750, the only eutectic ceramic in which superplastic behaviour was detected, hinders the dislocation activity whereas facilitates the mass transport by diffusion. This result is in agreement with a recent study performed in Al_2O_3–$Er_3Al_5O_{12}$–ZrO_2 eutectic rods deformed in compression at elevated temperatures, where the creep resistance of the eutectics was found to decrease

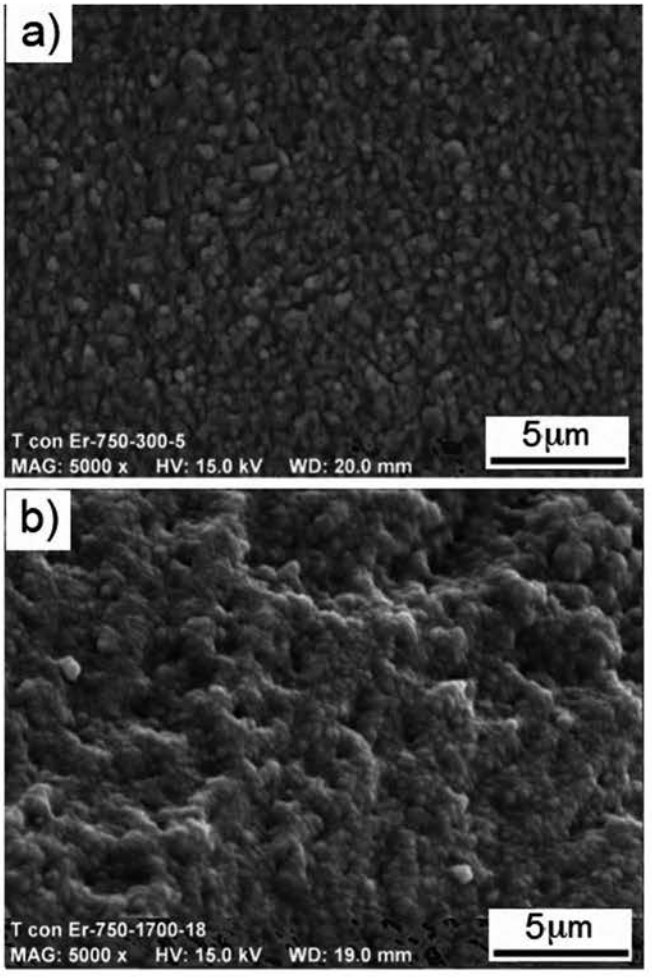

Fig. 8. Fracture surfaces of AEZ750 rods tested at (a) 300 K and (b) 1700 K.

with increasing the processing rate due to the microstructure refinement.[31] Moreover, further evidence of plastic deformation at 1700 K in the AEZ750 was found in the analysis of the fracture surfaces. They are shown in Fig. 8(a) and (b) for specimens tested at 300 K and 1700 K. It is difficult to decide whether crack propagation was transgranular or intergranular due to the small size of the eutectic domains but the fracture surface at 300 K was flat whereas plastic deformation at 1700 K was evidence by the roughness of the fracture surface.

4. Conclusions

Directionally solidified Al_2O_3–$Er_3Al_5O_{12}$–ZrO_2 eutectic rods were processed from the melt by the laser-heated floating zone method at different growth rates. The microstructure consisted of an interpenetrated network of the eutectic phases in which the phase size decreased rapidly as the growth rate increased. The hardness, fracture toughness and flexural strength were investigated as a function of the growth rate. Hardness and fracture toughness at room temperature were independent of the growth rate with average values of 15.6 GPa and 4 MPa $m^{1/2}$, respectively. The addition of ZrO_2 to the ternary eutectic improved the fracture toughness in a factor 2 compared

to the binary system. The increase of the fracture toughness in the ternary system has been previously found in the Al_2O_3–$Y_3Al_5O_{12}$–ZrO_2 eutectic. On the other hand, the flexural strength showed a large increase with the growth rate because of the microstructure refinement. Outstanding strength values of 3 GPa were measured at 750 mm/h, higher than those reported for the binary system. The influence of the temperature in the flexural strength was studied in all the samples up to 1900 K. A high strength retention was observed for the samples grown at 25 and 350 mm/h up to 1500 K. Above this temperature, the flexural strength showed an abrupt reduction. Superplastic behaviour was observed at 1700 K in the samples processed at the highest rate.

Acknowledgements

This study was funded by the Ministry of Science and Innovation under project MAT 2009-13979. M.C. Mesa would like to thank the Gobierno de Aragón for a grant. Authors acknowledge the use of Servicio de Microscopia Electrónica (Servicios de Apoyo a la Investigación), Universidad de Zaragoza.

References

1. Jackson KA, Hunt JD. Lamellar and rod eutectic growth. *Trans Met Soc AIME* 1966;**236**:1129–42.
2. LLorca J, Orera VM. Directionally-solidified eutectic ceramic oxides. *Prog Mater Sci* 2006;**51**:711–809.
3. Waku Y, Nakagawa N, Wakamoto T, Ohtsubo H, Shimizu K, Kohtoku Y. High temperature strength and thermal stability of a unidirectionally solidified Al_2O_3/YAG eutectic composite. *J Mater Sci* 1998;**33**: 1217–25.
4. Matson LE, Hecht N. Microstructural stability and mechanical properties of directionally solidified alumina/YAG eutectic monofilaments. *J Eur Ceram Soc* 1999;**19**:2487–501.
5. Ramírez-Rico J, Pinto-Gómez AR, Martínez-Fernández J, de Arellano-López AR, Oliete PB, Peña JI, et al. High-temperature plastic behaviour of Al_2O_3–$Y_3Al_5O_{12}$ directionally solidified eutectics. *Acta Mater* 2006;**54**:3107–16.
6. Waku Y, Sakata S, Mitani A, Shimizu K, Hasebe M. Temperature dependence of flexural strength and microstructure of $Al_2O_3/Y_3Al_5O_{12}/ZrO_2$ ternary melt growth composites. *J Mater Sci* 2002;**37**:2975–82.
7. Peña JI, Larsson M, Merino RI, de Francisco I, Orera VM, LLorca J, et al. Processing, microstructure and mechanical properties of directionally-solidied Al_2O_3–$Y_3Al_5O_{12}$–ZrO_2 ternary eutectics. *J Eur Ceram Soc* 2006;**26**:3113–21.
8. Pastor JY, Llorca J, Salazar A, Oliete PB, de Francisco I, Peña JI. Mechanical properties of melt-grown alumina–yttrium aluminum garnet eutectics up to 1900 K. *J Am Ceram Soc* 2005;**88**:1488–95.
9. Oliete PB, Peña JI, Larrea A, Orera VM, LLorca J, Pastor JY, et al. Ultra high strength nanofibrillar Al_2O_3–YAG–YSZ eutectics. *J Adv Mater* 2007;**19**:2313–8.
10. Nakagawa N, Ohtsubo H, Waku Y, Yugami H. Thermal emission properties of $Al_2O_3/Er_3Al_5O_{12}$ eutectic ceramics. *J Eur Ceram Soc* 2005;**25**:1285–91.
11. Waku Y, Nakagawa N, Ohtsubo H, Mitani A, Shimizu K. Fracture and deformation behaviour of melt growth composites at very high temperatures. *J Mater Sci* 2001;**36**:1585–94.
12. Mesa MC, Oliete PB, Orera VM, Pastor JY, Martín A, LLorca J. Microstructure and mechanical properties of $Al_2O_3/Er_3Al_5O_{12}$ eutectic rods grown by the laser-heated floating zone. *J Eur Ceram Soc* 2011;**31**:1241–50.
13. Mazerolles L, Perriere L, Lartigue-Korinec S, Piquet N, Parlier M. Microstructures, crystallography of interfaces and creep behaviour of melt-growth composites. *J Eur Ceram Soc* 2008;**28**:2301–8.
14. Martínez Fernández J, Sayir A, Farmer SC. High temperature creep deformation of directionally solidified $Al_2O_3/Er_3Al_5O_{12}$. *Acta Mater* 2003;**51**:1705–20.
15. Deng YF, Zhang J, Su HJ, Song K, Liu L, Fu HZ. Microstructure and fracture toughness of $Al_2O_3/Er_3Al_5O_{12}$ eutectic ceramic prepared by laser zone remelting. *J Inorg Mat Soc* 2011;**26**:841–6.
16. Mesa MC, Oliete PB, Larrea A. Microstructural stability at elevated temperatures of directionally solidified $Al_2O_3/Er_3Al_5O_{12}$ eutectic ceramics. *J Cryst Growth* 2012;**360**:119–22.
17. Waku Y, Sakata S, Mitani A, Shimizu K, Ohtsubo H, Hasebe M. Microstructure and high-temperature strength of $Al_2O_3/Er_3Al_5O_{12}/ZrO_2$ ternary melt growth composite. *J Mater Sci* 2005;**40**:711–7.
18. Oliete PB, Peña JI. Study of the gas inclusions in $Al_2O_3/Y_3Al_5O_{12}$ and $Al_2O_3/Y_3Al_5O_{12}/ZrO_2$ eutectic fibers grown by laser floating zone. *J Cryst Growth* 2007;**304**:514–9.
19. Mesa MC, Oliete PB, Larrea A, Orera VM. Directionally solidified Al_2O_3–$Er_3Al_5O_{12}$–ZrO_2 eutectic ceramics with interpenetrating or nanofibrillar microstructure: residual stress analysis. *J Am Ceram Soc* 2012;**95**:1138–46.
20. Larrea A, Orera VM, Merino RI, Peña JI. Microstructure and mechanical properties of Al_2O_3–YSZ and Al_2O_3–YAG directionally solidified eutectic plates. *J Eur Ceram Soc* 2005;**25**:1419–29.
21. Yang JM, Jeng SM, Chang S. Fracture behaviour of directionally solidified $Y_3Al_5O_{12}/Al_2O_3$ eutectic fiber. *J Am Ceram Soc* 1996;**79**(5):1218–22.
22. Lee JH, Yoshikawa A, Fukuda T, Waku Y. Growth and characterization of $Al_2O_3/Y_3Al_5O_{12}/ZrO_2$ ternary eutectic fibers. *J Cryst Growth* 2001;**231**:115–20.
23. Quinn GD, Bradt RC. On the Vickers indentation fracture toughness test. *J Am Ceram Soc* 2007;**90**:673–80.
24. Anstis GR, Chantikul P, Lawn BR, Marshall DB. A critical evaluation of indentation techniques for measuring fracture toughness. I. Direct crack measurements. *J Am Ceram Soc* 1981;**64**(9):533–8.
25. Niihara K, Morena R, Hasselman DPH. Evaluation of K_{IC} of brittle solids by the indentation method with low crack-to-indent ratios. *J Mater Sci Lett* 1982;**1**:13–6.
26. Gouadec G, Makaoui K, Perrière L, Colomban P, Mazerolles L. Ruby micro-piezospectroscopy in $GdAlO_3/Al_2O_3(/ZrO_2)$, $Er_3Al_5O_{12}/Al_2O_3(/ZrO_2)$ and $Y_3Al_5O_{12}/Al_2O_3(/ZrO_2)$ binary and ternary directionally solidified eutectics. *J Eur Ceram Soc* 2012;**3**:2145–51.
27. Perrière L, Valle R, Mazerolles L, Parlier M. Crack propagation in directionally solidified eutectic ceramics. *J Eur Ceram Soc* 2008;**28**:2337–43.
28. Pastor JY, LLorca J, Martín A, Peña JI, Oliete PB. Fracture toughness and strength of Al_2O_3–$Y_3Al_5O_{12}$ and Al_2O_3–$Y_3Al_5O_{12}$–ZrO_2 directionally solidified eutectic oxides up to 1900 K. *J Eur Ceram Soc* 2008;**28**: 2345–51.
29. Waku Y, Nakagawa N, Wakamoto T, Ohtsubo H, Shimizu K, Kohtoku Y. A ductile ceramic eutectic composite with high strength at 1873 K. *Nature* 1997;**389**:49–52.
30. Pastor JY, Martín A, Molina-Aldareguía JM, LLorca J, Oliete PB, Larrea A, et al. Superplastic deformation of directionally-solidified nanofibrillar Al_2O_3–$Y_3Al_5O_{12}$–ZrO_2 eutectics. *J Eur Ceram Soc* 2013;**33**:2579–86.
31. Huamán-Mamani FA, Jiménez-Melendo M, Mesa MC, Oliete PB. Microstructure and high-temperature mechanical behaviour of melt-grown $Al_2O_3/Er_3Al_5O_{12}/ZrO_2$ ternary eutectic composites. *J Alloys Compd* 2012;**M536S**:S527–31.